Journal of Applied Polymer Science

Preparation of Sn-doped CdS/TiO_2/conducting polymer fiber composites for efficient photocatalytic hydrogen production under visible light irradiation

Fengmei Ren,[1] Haihong Ma,[1] Wei Hu,[1,2] Zhengfa Zhou,[1] Weibing Xu[1]

[1]Department of Polymer Science and Engineering, Hefei University of Technology, Hefei, Anhui 230009, People's Republic of China

[2]Anhui Province Testing Center of Packaging Products Quality Supervision, Tongcheng, Anhui 231400, China

Correspondence to: W. Xu (E-mail: weibingxu@hfut.edu.cn)

ABSTRACT: Sn-doped CdS/TiO_2 heterojunction was synthesized on the conducting polymer fiber mat by hydrothermal method. The conducting polymer fiber mat was made by electrospinning from polyvinylidene fluoride, styrene-maleic anhydride copolymer, and nano-graphites as conducting fillers. The Sn-doped CdS/TiO_2 heterojunction was characterized by XRD, XPS, SEM, TEM, TGA, and UV–Vis absorption spectra. Under simulated solar light irradiation, a combination of Sn-doped CdS/TiO_2/conducting polymer was found to be highly efficient for photocatalytic hydrogen evolution from splitting of water. The photocatalytic hydrogen production efficiency was up to 2885 μmol h^{-1} g^{-1}cat. © 2015 Wiley Periodicals, Inc. J. Appl. Polym. Sci. **2015**, *132*, 42300.

KEYWORDS: catalysts; composites; fibers

Received 3 December 2014; accepted 4 April 2015

DOI: 10.1002/app.42300

INTRODUCTION

The development of human society based on fossil fuels results in a significant negative impact on environment. Clean renewable energy sources are desiderata for mankind. Solar energy is one of clean renewable energy sources. The conversion of solar energy into chemicals to generate solar fuels should be the most promising proposition of the global energy crisis.[1,2] Photocatalytic water splitting has been a focus topic because it provides a promising way of utilizing solar energy to produce hydrogen on large scale.[3] There are many semiconductors have been used for photocatalytic hydrogen producing. Many wide-band-gap oxide photocatalysts, such as TiO_2[4] and ZnO,[5] can only absorb the UV light, merely about 5% of the solar spectrum. While narrow-gap photocatalysts, such as CdS,[6,7] are not photostable and undergoes photocorrosion. So the development of efficient visible-light-responsive stable photocatalysts is indispensable to full utilization of the solar light.

A great variety of strategies have been adopted to enhance the efficiency of light harvesting and solar energy converting. The two great approaches are to narrow band gap and increase surface area of catalysts. To narrow band gap can enhance light harvesting, introduce active sites for reaction, and suppress recombination of photogenerated electron–hole pairs. Band gap gets narrow through doping transition metal cations,[8] loading co-catalysts,[9] dye sensitization,[10] doping anion,[11,12] and coupling semiconductor.[13,14] Increasing surface area by constructing nano- or mesostructured materials can introduce more active sites for reaction and prolong efficient light path to enhance light harvesting.[15–18]

Recent studies have adopted both methods to improve the efficiency of photocatalysts. Yu *et al.*[13] found self-assembly of the 10 wt % TiO_2/CdS mesoporous microspheres showed improved stability. The mesoporous structure could increase the utilization of light energy and facilitate the diffusion of reactants and products during the photocatalytic reaction for the degradation of RhB. Yu *et al.*[14] engineered interfacial nanostructures in Bi_2S_3-TiO_2 nanorod-nanoparticle heterostructures. TiO_2 nanoparticles was grown on the {310} facet of the preprepared Bi_2S_3 nanorods with interfacial defects. The defect-free interfaces favored electron–hole separation and transfer, resulting in improved photocatalytic activity. Zhou *et al.*[19] designed leaf-inspired hierarchical porous CdS/Au/N-TiO_2 heterostructures systems. The hierarchical macro/mesoporous morphology and CdS(shell)/Au(core)/N-TiO_2 heterostructures modules could enhance overall light harvesting and offer more reaction sites for the catalysis. The hydrogen evolution rates of optimized leaf-inspired hierarchical porous CdS (3.04 wt %)/Au/N-TiO_2 three-component heterostructures are about 270 times that of

Au/N-TiO_2 under visible light irradiation. Yu *et al.*[8] discussed nanorod-like Pt-modified CdS/TiO_2 samples. The results indicated that the as-prepared samples exhibited 106.3 times higher activities than pure TiO_2 in the evolution of hydrogen under simulated solar light irradiation.

Researchers found that the $SnS_x(x = 1,2)/TiO_2$ composites were visible-light-responsive,[20] SnS_2/SnO_2 nanocomposites with suitable SnO_2 contents had remarkable photocatalytic stability,[21] CdS decorated Sb-SnO_2/TiO_2-NTs hybrid electrode enhances the conductivity of TiO_2, owing to faster charge transport and more efficient charge separation of Sb–SnO_2.[22]

To narrow the gap of photocatalyst, we use facile and cheap tin compounds to replace noble metal to decorate CdS and TiO_2 heterogeneous, and use conducting electrospinning polymer fibers to carry the heterogeneous photocatalyst. The electrospinning polymer fibers could prevent the agglomeration of photocatalysts nanoparticle.[23–25] The conducting polymer fibers could enhance the separation of photogenerated electron–hole pairs, and increase the efficiency of photocatalysis.[26–28]

Sn-doped CdS/TiO_2/conducting polymer fiber composites was evaluated to photocatalytic hydrogen evolution from splitting of water under simulated solar light irradiation. In order to enhance photocatalytic activity, tin ions were doped into CdS particles which were synthesized on the conducting polymer fiber mat. Then the Sn doping CdS particles were covered with TiO_2 for making core–shell structural heterojunction. The present investigation provides a cost-effective method for hydrogen evolution from splitting of water.

EXPERIMENTAL

Materials

Polyvinylidene fluoride (PVDF) was supplied by Solvay Solexis. Nano-graphites (40 nm) was purchased from Nanjing XFNANO Materials Tech. Titanyl sulfate ($TiOSO_4$) was obtained from Dandong Zhongxing Chemical Factory. Styrene-maleic anhydride copolymer (SMA), cadmium chloride ($CdCl_2{\cdot}2.5H_2O$), stannic chloride ($SnCl_4$), thiourea ($(NH_2)_2CS$) and other chemicals were bought from Shanghai Chemicals. All materials were used as received.

Electrospinning of Conducting Polymer Fiber Mats

Conducting polymer fiber mats were prepared in a typical electrospinning process. PVDF (3.6 g), SMA (0.41 g) and conductive nano-graphite (0.4 g) were added into the mixture of acetone (14.0 mL) and *N*, *N*-dimethylacetamide (20.0 mL). After stirring for 24 h, the solution was electrospun at 25 kV positive voltage, 18 cm working distance (between the target and the needle tip), and 1.2 mL/h flow rate. All process steps were operated at room temperature. Conducting polymer fiber mats were cut into strips of 5.0 cm × 5.0 cm in dimension for the succedent experiments.

As a comparative experiment, nonconducting polymer fiber mats were synthesized by the same method without adding conductive nano-graphite.

Preparation of Sn-Doped CdS/Conducting Polymer Fiber Composites

The as-prepared electrospun conducting polymer fiber mats were put into the aqueous solution of $CdCl_2$ and $SnCl_4$ (20 mL, 0.25 mol/L, the ratio of Cd^{2+} to Sn^{4+} is 1 to 1) for 12 h to form the complex between carboxyls of polymer fiber and the Cd^{2+} and Sn^{4+}. Subsequently the fiber mats were immersed into a 50 mL teflon-lined stainless steel autoclave including desired concentration of $(NH_2)_2CS$ (20 mL, 0.25 mol/L). The autoclave was placed in an oven for 12 h at 120°C, and then it was cooled to room temperature in the air. The Sn-doped CdS/conducting polymer fiber composites were washed with distilled water under ultrasonic vibrations in order to remove the byproducts and unreacted precursor, and were dried in vacuum for 3 h at 60°C.

Preparation of Sn-Doped CdS/TiO_2/Conducting Polymer Fiber Composites

Then as-prepared Sn-doped CdS/conducting polymer fiber composites were immersed into desired concentration $TiOSO_4$ (40 mL, 0.5 mol/L) aqueous solution for 12 h. Subsequently, the solution with the composites was put in teflon-lined stainless steel autoclave. The autoclave was places in an oven for 12 h at 120°C, and then it was cooled down to room temperature in the air. The Sn-doped CdS/TiO_2/conducting polymer fiber composites were washed, dried as the previous step.

As a comparative experiment, Sn-doped CdS/TiO_2/nonconducting polymer fiber composites were synthesized by the similar method without adding conductive nano-graphite, and CdS/TiO_2/conducting polymer fiber composites were synthesized by the similar method without adding $SnCl_4$. In the remainder of this article, the Sn-doped CdS/TiO_2/conducting polymer fiber composites were shortened to composites SCP, for convenience. And the composites without adding conductive nano-graphite and composites without doping Sn were shortened to composites SP and composites CP, respectively.

Photocatalytic Reaction

Photocatalytic activities of the as-prepared samples for generation of hydrogen were carried in SGY-IB multipurpose chemical reactor from Nanjing Sionetech Electrical Equipment, the light source was xenon lamp (350 W), and the reaction system temperature was kept at 25 ± 1°C using flowing cool water to remove the heat generated by Xe lamp. Composites SCP (0.294 g containing 0.059 g Sn-doped CdS/TiO_2) and composites SP (0.577 g containing 0.102 g Sn-doped CdS/TiO_2) were added separately in an aqueous solution (250 mL) containing Na_2S (0.25 mol/L) and Na_2SO_3 (0.35 mol/L) with a magnetic stirrer. While the composites CP (0.340 g containing 0.092 g CdS/TiO_2) were added separately in the same solution. The system was initially purged by N_2 in dark environment to exclude the oxygen.

Characterization

Field-emission scanning electron microscopy (FE-SEM) was carried out with a JSM-6490LV. High-resolution transmission electron microscope(HRTEM) image and the selected area electron diffraction (SAED) pattern were taken on JEM-2100. The X-ray diffraction (XRD) (Rigaku D/max-β B, Rigku Corporation, Japan) measurement was carried out using a Cu-K*a* radiation source. X-ray photoelectron spectroscopy (XPS) spectra were detected by the ESCALAB-MK-II. Diffuse reflectance ultraviolet–visible (UV–Vis) absorption spectra were measured at room temperature in the range from 230 to 800 nm on a Shimadzu

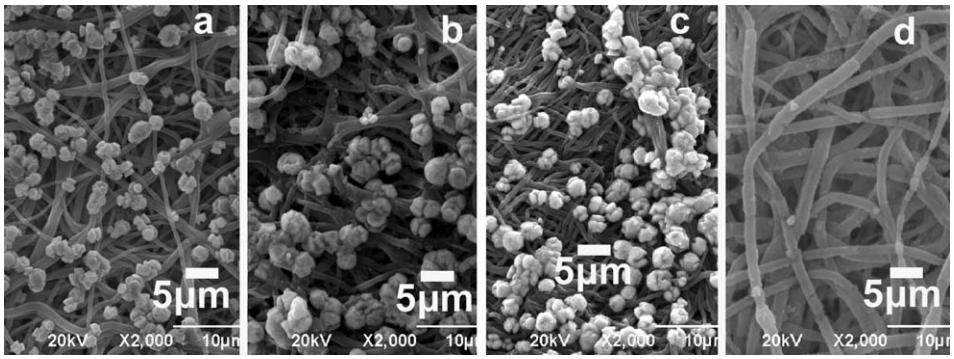

Figure 1. SEM images of (a) Sn-doped CdS/conducting polymer fiber composites, (b) composites SCP, (c) composites SP, and (d) composites CP.

Solidspec-3700 DUV spectrophotometer, and $BaSO_4$ was used as a reference in each measurement.

The thermogravimetric analysis (TGA) was employed to estimate the weight loss of composites on Netzsch TG-209-F3 at a scan rate of 10°C min^{-1} from 35 to 800°C under N_2. The amount of hydrogen production was measured by gas chromatography (SP-6801, N_2 carrier).

RESULTS AND DISCUSSION

Structure and Morphology of Composites

Figure 1 illustrated the SEM images of Sn-doped CdS/conducting polymer fiber composites [Figure 1(a)], composites SCP [Figure 1(b)], composites SP [Figure 1(c)], composites CP [Figure 1(d)]. The spherical Sn-doped CdS particles of about 1 to 2 μm in diameter grew on the surface of fibers. The Sn-doped CdS particles were covered with TiO_2 microparticles, and the diameter of the heterogeneous particles was about 2–3 μm. The dimension and morphology of composites SP were similar to those of composites SCP. The CdS wrapt around the conducting polymer fiber was covered with TiO_2 as the thickness of the CdS/TiO_2 was about 800 nm. The HRTEM images of composites SCP demonstrated that area X was the fiber with the diameter of about 600 nm, and area Y was the inorganic matter, as shown in Figure 2(a). The selected area in Figure 2(a) was inclusive of two types of nanocrystallites with indistinct polygonal shape as shown in Figure 2(b). The SAED pattern of Sn-doped CdS/TiO_2 nanocrystallite was indistinct rings as shown in Figure 2(c), which is further analyzed by XRD in Figure 3. The content of Sn-doped CdS/TiO_2 in composites SCP and composites SP, which confirmed by TGA, were 20, 17.7%, respectively. While the content of CdS/TiO_2 in composites CP was 27.0%.

Figure 3 showed the XRD patterns of composites SCP, composites SP and composites CP. The diffraction peak located at 26.5° (2θ

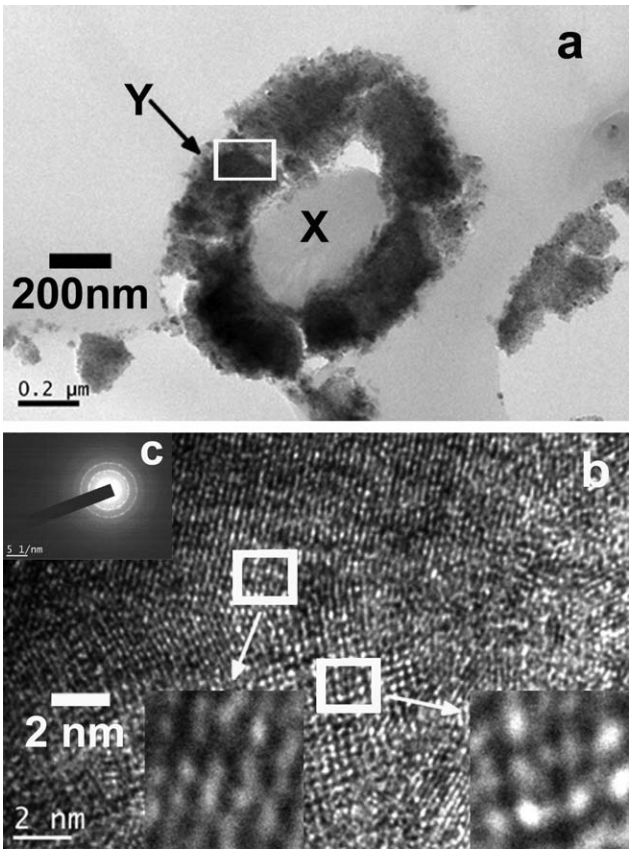

Figure 2. HRTEM images of (a) composites SCP, (b) enlarged image, and (c) SAED of the sample.

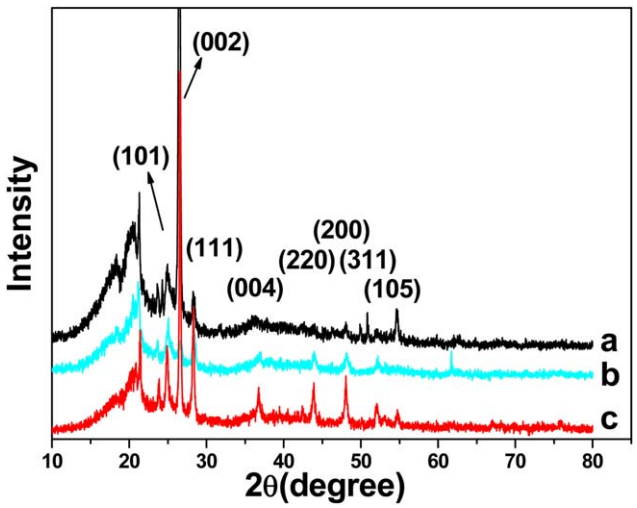

Figure 3. XRD patterns of (a) composites SCP, (b) composites SP, and (c) composites CP. [Color figure can be viewed in the online issue, which is available at wileyonlinelibrary.com.]

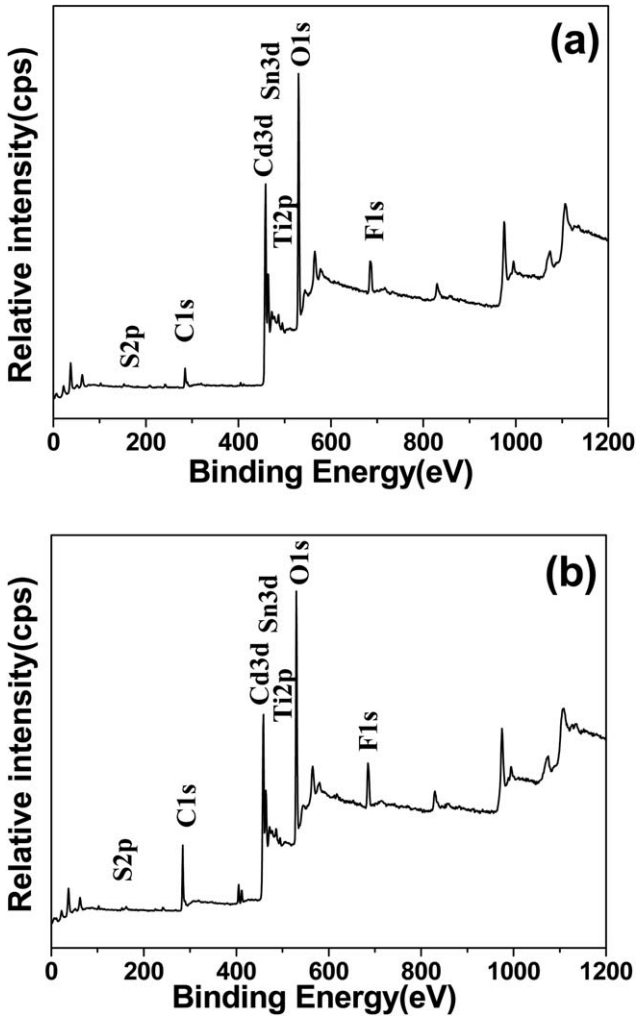

Figure 4. XPS spectra of (a) composites SCP and (b) composites SP.

value in Figure 3(a–c) corresponded to (002) *graphite* phase (JCPDS card No. 26–1079). The diffraction peak at 25.7°, 37.8°, 48.0°, 53.8° corresponded to (101), (004), (200), (105) planes of the anatase structure of TiO_2 (JCPDS card No. 21–1272).[20] The diffraction peaks at 28.4°, 43.8°, 52.5° corresponded to (111), (220), (311) planes of the cubic structure of CdS (JCPDS card No. 10–0454).[8] The diffraction peaks, which corresponded to planes of the hexagonal structure of CdS, were not so obvious. It is indicted that CdS nanocrystals are mixtures of cubic phase and a little of hexagon phase.

Comparing with composites CP, the diffraction peaks in composites SCP, which corresponded to (220) and (311) planes, were not so obvious. This may be resulted from the effect of tin ions in the crystallization of CdS. The indistinct rings of the SAED pattern of Sn-doped CdS/TiO_2 nanocrystallite illustrated the crystallization was imperfect.

XPS spectra of composites SCP and composites SP were shown in Figure 4(a,b), respectively. The spectra demonstrated that the two composites were composed of C, O, F, Cd, Sn, Ti, and S elements, which were corresponding to composites SCP and composites SP.

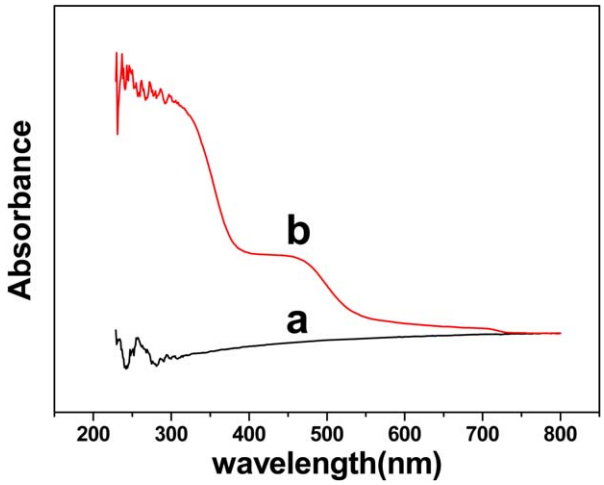

Figure 5. UV/VIS absorption spectra of (a) conducting polymer fiber composites and (b) composites SCP. [Color figure can be viewed in the online issue, which is available at wileyonlinelibrary.com.]

Ultraviolet–Visible Absorption Spectra

The conducting polymer electrospun mats have no evident absorption above 260 nm [Figure 5(a)], while composites SCP have absorption peak sat round 440 and 600 nm [Figure 6(b)]. This reveals that the conducting polymer electrospun mats do not interfere with the light absorption of Sn-doped CdS/TiO_2 of composites SCP during the photocatalytic reaction. Compared with the absorption peaks of pulverous TiO_2 and CdS, which emerged at 400 and 550 nm,[19] the absorption peaks of Sn-doped conducting polymer fiber composites have strong absorption in the visible light region(from 440 to 600 nm). The doped tin ions were formed into tin sulfides. SnS has a narrow band gap of about 1.32 eV, SnS_2 has a larger band gap of about 2.35 eV.[29] The addition of SnS and SnS_2 narrow the band gap of CdS/TiO_2 heterojunction.

Photocatalytic Activity of Generation of Hydrogen

The photocatalytic generation of hydrogen from water was determined using composites SCP as photocatalyst, and

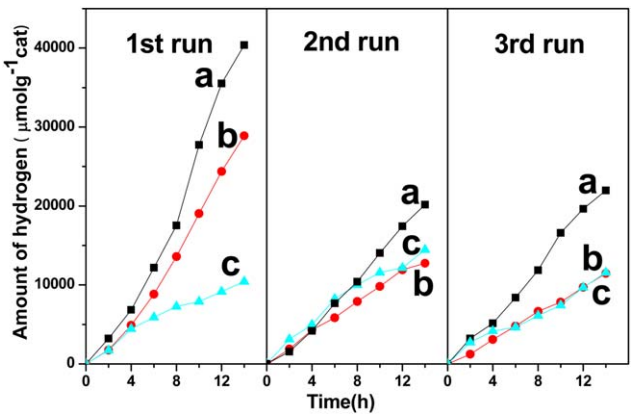

Figure 6. Photocatalytic hydrogen evolution of (a) composites SCP, (b) composites SP, and (c) composites CP. [Color figure can be viewed in the online issue, which is available at wileyonlinelibrary.com.]

compared with composites SP and composites CP. The uptake rate of hydrogen from water experiments was carried out based on the average value obtained from three respective runs. For each run, the photocatalytic reaction was made for 14 h and the concentration of sacrificial agents (Na_2SO_3 and Na_2S) was kept identical. The experiment results were shown in Figure 6. The average rate of hydrogen generation of composites SCP was higher than that of composites SP and composites CP. In the three runs, the average rate of hydrogen evolution of composites SCP, which is 2885, 1440, and 1567 μmol h^{-1} g^{-1}cat, respectively, was higher than that of the others. And that of composites SP and composites CP was 2064, 910, and 818 μmol h^{-1} g^{-1}cat and 745, 1031, and 825 μmol h^{-1} g^{-1} cat, respectively. In the first run, the average rate of hydrogen generation of composites SCP was 1.40 times that of composites SP and 3.86 times that of composites CP. In the third run, the average rate of hydrogen evolution of composites SCP was 1.9 times that of the other two composites. For comparison, the average rate of hydrogen generation of leaf-inspired hierarchical porous CdS (3.04 wt %)/Au/N-TiO_2 heterostructures was 92 μmol h^{-1}g cat^{-1}, illuminated by 750 W Xe lamp, using the same sacrificial reagent (0.25 mol/L Na_2S and 0.35 mol/L Na_2SO_3) as ours,[19] and that of nanorod-like Pt-modified CdS(10%)/TiO_2 was 1063 μmol h^{-1}g cat^{-1}, illuminated by 500 W Xe lamp, using the same sacrificial reagent.[8]

There are two possible reasons for this phenomenon. Firstly, when Sn^{4+} ion was doped into the CdS of the fibers, the band gap of the catalyst narrowed and has high-energy efficiency of visible light irradiation. Secondly, the photogenerated electron–hole pairs within Sn-doped CdS/TiO_2 were produced in the light, the electron migrate to the surface of Sn-doped CdS/TiO_2 and generate hydrogen by the reduction of water. Because the fiber has some electrical conductivity, it is easy for holes to migrate to the fiber, which result in the separation of the electron–hole pairs and therefore improve the photocatalytic efficiency.

CONCLUSION

In summary, novel composites photocatalysts—composites SCP, SP, and CP-Sn-doped CdS/TiO_2/conducting polymer fiber composites were successfully synthesized. Doping of Sn and the conductivity of carriers had an obvious effect on enhancing the photocatalytic efficiency of semiconducting photocatalysts. The average rate of hydrogen evolution from water using composites SCP was higher than that using composites SP and composites CP from the first run to the third run. In the first run, the average rate of hydrogen generation of composites SCP was 1.40 times that of composites SP and 3.86 times that of composites CP. In the third run, the average rate of hydrogen evolution of composites SCP was 1.9 times that of the other two composites. These novel photocatalytic composites have great potential in clean renewable energy field.

ACKNOWLEDGMENTS

The authors thank The National Natural Science Foundation of China (20776034) and The Natural Science Fund of Anhui Provincial Education Department (KJ2010B198) for the support of this work.

REFERENCES

1. Tong, H.; Ouyang, S.; Bi, Y.; Umezawa, N.; Oshikiri, M.; Ye, J. *Adv. Mater.* **2012**, *24*, 229.
2. Osterloh, F. E. *Chem. Mater.* **2008**, *20*, 35.
3. Kudo, A.; Miseki, Y. *Chem. Soc. Rev.* **2009**, *38*, 253.
4. Peng, S. Q.; Li, Y. X.; Jiang, F. Y.; Lu, G. X.; Li, S. B. *Chem. Phys. Lett.* **2004**, *398*, 235.
5. Graifer, A. Y.; Koshcheev, A. P.; Myasnikov, I. A. *Kinet. Catal.* **1988**, *28*, 1137.
6. Li, Y. X.; Hu, Y. F.; Peng, S. Q.; Lu, G. X.; Li, S. B. *J. Phys. Chem. C* **2009**, *113*, 9352.
7. Li, Q.; Guo, B. D.; Yu, J. G.; Ran, J. R.; Zhang, B. H.; Yan, H. J.; Gong, J. R. *J. Am. Chem. Soc.* **2011**, *133*, 10878.
8. Yu, Q.; Xu, J.; Wang, W. Z.; Lu, C. L. *Mater. Res. Bull.* **2014**, *51*, 40.
9. Antony, R. P.; Mathews, T.; Ramesh, C.; Murugesan, N.; Dasgupta, A.; Dhara, S.; Dash, S.; Tyagi, A. K. *Int. J. Hydrogen Energy* **2012**, *37*, 8268.
10. Zyoud, A.; Zaatar, N.; Saadeddin, I.; Helal, M. H.; Campet, G.; Hakim, M.; Park, D.; Hilal, H. S. *Solid State Sci.* **2011**, *13*, 1268.
11. Liu, M. C.; Du, Y. C.; Ma, L. J.; Jing, D. W.; Guo, L. *J. Int. J. Hydrogen Energy* **2012**, *37*, 730.
12. Peng, S. Q.; Chen, C. H.; Liu, X. Y.; Li, Y. X. *React. Kinet. Mech. Catal.* **2013**, *110*, 259.
13. Yu, S. J.; Hu, J. C.; Li, J. L. *Int. J. Photoenergy* **2014**, DOI: 10.1155/2014/854217.
14. Yu, H. J.; Huang, J.; Zhang, H.; Zhao, Q. F.; Zhong, X. H. *Nanotechnology* **2014**, DOI:10.1088/0957-4484/25/21/215702.
15. D'Elia, D.; Beauger, C.; Hochepied, J. F.; Rigacc, A.; Bergerc, M. H.; Keller, N.; Keller, S. V.; Suzuki, Y.; Valmalette, J. C.; Benabdesselam, M.; Achard, P. *Int. J. Hydrogen Energy* **2011**, *36*, 14360.
16. Liu, Z.; Bai, H.; Xu, S.; Sun, D. D. *Int. J. Hydrogen Energy* **2011**, *36*, 13473.
17. Nakane, K.; Yasuda, K.; Ogihara, T.; Ogata, N.; Yamaguchi, S. *J. Appl. Polym. Sci.* **2007**, *104*, 1232.
18. Gong, L. X.; Zhou, Z. F.; Wang, S. M.; Wang, B. *J. Appl. Polym. Sci.* **2013**, *129*, 1212.
19. Zhou, H.; Liang, D.; Fan, T. X.; Ding, J.; Zhang, D.; Guo, Q. X. *Appl. Catal. B: Environ.* **2014**, *147*, 221.
20. Yang, C. Y.; Wang, W. D.; Shan, Z. C.; Huang, F. Q. *J. Solid State Chem.* **2009**, *182*, 807.
21. Zhang, Y. C.; Du, Z. N.; Li, K. W.; Zhang, M.; Dionysiou, D. D. *ACS Appl. Mater. Interface* **2011**, *3*, 1528.
22. Zhang, Q.; Xu, H.; Yan, W. *Electrochim. Acta* **2012**, *61*, 64.
23. Agarwal, S.; Greiner, A.; Wendorff, J. H. *Prog. Polym. Sci.* **2013**, *38*, 963.

24. Ye, S. H.; Zhang, D.; Liu, H. Q.; Zhou, J. P. *J. Appl. Polym. Sci.* **2011**, *121*, 1757.

25. Costa, R. G. F.; Ribeiro, C.; Mattoso, L. H. C. *J. Appl. Polym. Sci.* **2013**, *127*, 4463.

26. Fan, W. J.; Zhou, Z. F.; Xu, W. B.; Shi, Z. F.; Ren, F. M.; Ma, H. H.; Huang, S. W. *Int. J. Hydrogen Energy* **2010**, *35*, 6525.

27. He, T. S.; Zhou, Z. F.; Xu,W. B.; Ren, F. M.; Ma, H. H.; Wang, J. *Polymer* **2009**, *50*, 3031.

28. Ren, F. M.; Hu, W.; Zhou, Z. F.; Ma, H. H.; Xu,W. B. *Optoelectron. Adv. Mat. Rapid Commun.* **2014**, *8*, 858.

29. Gou, X. L.; Chen, J.; Shen, P. W. *Mater. Chem. Phys.* **2005**, *93*, 557.